Reconstruction-Based Recognition of Scenes with Translationally Repeated Quadrics

Ragini Choudhury, J.B. Srivastava, and Santanu Chaudhury, *Member*, *IEEE*

Abstract—This paper addresses the problem of invariant-based recognition of quadric configurations from a single image. These configurations consist of a pair of rigidly connected translationally repeated quadric surfaces. This problem is approached via a reconstruction framework. A new mathematical framework, using relative affine structure, on the lines of Luong and Vieville [12], has been proposed. Using this mathematical framework, translationally repeated objects have been projectively reconstructed, from a single image, with four image point correspondences of the distinguished points on the object and its translate. This has been used to obtain a reconstruction of a pair of translationally repeated quadrics. We have proposed joint projective invariants of a pair of proper quadrics. For the purpose of recognition of quadric configurations, we compute these invariants for the pair of reconstructed quadrics. Experimental results on synthetic and real images, establish the discriminatory power and stability of the proposed invariant-based recognition strategy. As a specific example, we have applied this technique for discriminating images of monuments which are characterized by translationally repeated domes modeled as quadrics.

Index Terms—3D objects, reconstruction, recognition, projective invariants, translationally repeated objects, quadrics.

1 Introduction

In this paper, we have addressed the problem of recognition of scenes composed of translationally repeated quadrics. Quadrics have been assumed to be rigidly placed, that is, the translation between the quadrics is fixed. Quadrics are 3D shapes like ellipsoids, hyperboloids, etc. They can occur as individual objects or as parts of more complex objects. There are many examples of real 3D scenes where each of these objects are configured in a repeated manner. Historical monuments of architectural significance, with multidome structure (Figs. 6, 7, and 8), are typical examples of such scene configurations, where each of the domes can be modeled as a quadric (ellipsoid) (Fig. 9). The proposed recognition scheme involves a projective reconstruction of the quadrics from a single image of the scene and computation of projective invariants for a pair of proper quadrics. We have carried out experimental investigations on synthetic and real images, to study the discriminatory power and the stability of the invariant-based recognition strategy. We have applied this technique for identification of historical monuments and have received encouraging results.

Invariant-based recognition schemes for 3D objects are appealing because invariants provide viewpoint independent descriptors of these objects. However, unlike planar objects [19], [8], [10], [16], [17], [18], it is not possible to formulate invariants for the general class of 3D objects [24]. Invariants of only specific classes of 3D objects can be computed from a single image, by exploiting certain class specific geometric constraints [2], [24], [15]. Translationally repeated objects and algebraic surfaces are two such classes. Quadrics are algebraic surfaces. In this paper, we explore a combination of these classes in the form of translationally repeated objects in which each of the components is a quadric and exploit the geometric constraint of repetition. In this paper, we have proposed a reconstruction-based recognition strategy for translationally repeated objects and applied it specifically to the case of translationally repeated quadrics given a single image of a repeated object. The proposed recognition scheme uses joint projective invariants computed from the pair of reconstructed quadrics. This approach for recognition of translationally repeated quadrics via projectively reconstructed quadric components is the unique contribution of the paper as such reconstruction-based recognition schemes are few in the literature [24]. In fact, the recognition strategy is general and applicable to all repeated objects for which invariants can be computed.

Work on repeated objects in the past has concentrated on their reconstruction, handled by converting a single image to the equivalent multiple view of the single instance. This has lead to the convergence of the single view [13], [14] and multiple view-based approaches [7], [20]. The affine structure for translationally repeated objects has been obtained by Moons et al. [13] using vanishing points and five point correspondences between the two views. Mundy and Zisserman [14] have studied affine structure as a projective ambiguity matrix. Shashua [21], [22] has handled affine structure as a special case of relative affine structure. By exploiting this affine ambiguity, Liu et al. [11] obtained 3D affine invariants for recognizing 3D translationally

- *R. Choudhury is with INRIA Rhône-Alpes, ZIRST-655 avenue de l'Europe, 38330 Montbonnot, St. Martin, France. E-mail: Ragini.Choudhury@inrialpes.fr.*
- *J.B. Srivastava is with the Department of Mathematics, IIT, Delhi , Hauz Khas, New Delhi 110016, India. E-mail: jbsrivas@maths.iitd.ernet.in.*
- *S. Chaudhury is with the Department of Electrical Engineering, IIT Delhi, Hauz Khas, New Delhi 110016, India. E-mail: santanuc@cse.iitd.ernet.in.*

Manuscript received8 Mar. 2000; revised 17 Oct. 2000; accepted 12 Dec. 2000.
Recommended for acceptance by P Flynn.
For information on obtaining reprints of this article, please send e-mail to: tpami@computer.org, and reference IEEECS Log Number 111661.

repeated objects. But, affine structure does not suffice for an extension to reconstruction scheme for translationally repeated quadrics. Therefore, the technique of [11] is not applicable to quadric configurations in our context.

We first develop a new framework for the relative affine reconstruction of translationally repeated objects from a single uncalibrated image by converting it to its equivalent stereo image framework where the second camera is a translate of the original camera. This reconstruction scheme, in fact, is general and applicable to different classes of translationally repeated objects. It requires the knowledge of four image point correspondences on the object and its translate, and the choice of four points is not critical to the strategy. A new mathematical framework has been proposed for transforming a pair of uncalibrated cameras such that the first camera gets aligned. The second camera matrix involves a homography between two image planes and a normalized second epipole, both of which are computable from image information. Although relative affine structure has been obtained in the past [21], [12] using two images of the object, the novelty in the contribution of our paper lies in the modifying the existing formulation and developing the theory which handles reconstruction of repeated objects from a single image. Reconstructing the translated component from the available information has not been handled in the past.

In the particular case of applying the above scheme to reconstruct translationally repeated quadrics, we require additional information of the outline conics. The relative affine structure has been necessitated by quadric reconstruction. Although Shashua and Toelg [23] and Cross and Zisserman [6] have reconstructed quadrics using two views, they do not address the problem of repeated objects. Shashua and Toelg [23] reconstructed a quadric reference surface using the knowledge of outline conic and four point correspondences in the two images. Cross and Zisserman [6] do a quadric reconstruction using dual space geometry. Repeated applications of these strategies, either by taking both the components together or by reversing the camera set up, will lead to components which are reconstructed with respect to different frames and, hence, cannot be used for computing joint invariants essential for recognition. Our reconstruction framework overcomes this difficulty by incorporating the repetitions in the same frame.

The invariants computed using these reconstructed quadrics have the ability to distinguish quadric configurations on the basis of translation between the quadrics and the nature of quadrics. Consequently, the invariants are appropriate for recognition of different configurations like historical monuments which are distinguished by the location of repeated quadrics and the nature of quadrics. The occurrence of multiple quadrics and the relatively large separation between the quadrics on the actual structures make this approach robust against occlusion. An alternate framework to handle occlusion specifically has been developed using the repetition explicitly [4].

The paper is organized as follows: In Section 2, we define the problem and give the mathematical background required for the paper and give the projective ambiguity matrix used in reconstruction. Section 3 gives a projective reconstruction of translationally repeated objects, in general. In Section 4, we have reconstructed a pair of translationally repeated quadrics. Section 5 deals with the computation of joint projective invariants for an arbitrary pair of proper quadrics. These invariants are then used for the purpose of recognition of quadric configurations. Section 6 contains experimental results regarding discriminatory power and the stability of the strategy. Implementation has been done on synthetic and real images. The applications of the theory developed have been carried out for the special case of famous historical monuments, which contain translationally repeated domes. This is followed by a section which gives the conclusions. Finally, the Appendix contains the proofs of some of the theorems referred to in the paper.

2 Problem Definition and Approach to Solution

Our aim in the paper is to recognize translationally repeated 3D objects. They consist of components S and S' such that $S' = T(S)$, where

$$T = \begin{bmatrix} I_3 & \mathbf{t} \\ 0 & 1 \end{bmatrix}, \ \mathbf{t} = (t_1\ t_2\ t_3)^t$$

denotes translation. Such objects are called *Translationally repeated objects*. With this end in view, we propose a reconstruction-based recognition strategy for such objects. We will first reconstruct the two components with respect to the same frame and use these to compute the values of the projective invariants. These values are used for the purpose of recognition.

The recognition and reconstruction of translationally repeated objects is handled by converting the single camera framework to its equivalent stereo framework. A *camera* here means a perspective uncalibrated camera represented by a 3×4 matrix of the form $[P\ p]$ with $\det(P) \neq 0$ and centre of perspectivity (COP) in homogeneous coordinates given by

$$\begin{pmatrix} -P^{-1}p \\ 1 \end{pmatrix}.$$

Let $\widetilde{P} = [P\ p]$ and $\widetilde{P}' = [P'\ p']$ represent two cameras in the equivalent stereo framework with respective center of perspectivities given by

$$COP_1 = \begin{pmatrix} -P^{-1}p \\ 1 \end{pmatrix} \text{ and } COP_2 = \begin{pmatrix} -P'^{-1}p' \\ 1 \end{pmatrix}$$

and having respective image planes $\mathcal{R}_1$ and $\mathcal{R}_2$.

Let $M = (X\ Y\ Z\ 1)^t$ represent an arbitrary 3D point in homogeneous coordinates. Define

$$\widetilde{m} = [P\ p]M = z_M \begin{pmatrix} x_M/z_M \\ y_M/z_M \\ 1 \end{pmatrix} = \lambda m,$$

$\lambda = z_M \neq 0$ and $m = (x\ y\ 1)^t$ is observable in the image. Similarly, $\widetilde{m}' = [P'p']M = \lambda' m', \lambda' \neq 0, m' = (x'\ y'\ 1)^t$, where m' is observable in the image. By definition, m and m' or $\widetilde{m}$ and $\widetilde{m}'$ are said to be *corresponding points*.

The epipoles are defined as

$$\widetilde{e} = [P\ p]\begin{pmatrix} -P'^{-1}p' \\ 1 \end{pmatrix} = \lambda_e e,\ \ e = \begin{pmatrix} e_1 \\ e_2 \\ 1 \end{pmatrix}$$

and

$$\widetilde{e}' = [P'\ p']\begin{pmatrix} -P^{-1}p \\ 1 \end{pmatrix} = \lambda_{e'} e',\ \ e' = \begin{pmatrix} e'_1 \\ e'_2 \\ 1 \end{pmatrix}.$$

We now define the homography H_Π from image plane $\mathcal{R}_1$ to the image plane $\mathcal{R}_2$. Let Π be a plane which does not contain COP_1 and COP_2. Let $h_1 = [P\ p]|_\Pi : \Pi \rightarrow \mathcal{R}_1$ and $h_2 = [P'\ p']|_\Pi : \Pi \rightarrow \mathcal{R}_2$ denote the restriction of $[P\ p]$ and $[P'\ p']$ to the plane Π, respectively. This means $h_1 M = [P\ p]M$ and $h_2 M = [P'\ p']M$ for every $M \in \Pi$. Since COP's do not belong to Π, both h_1 and h_2 are invertible. Define $H_\Pi : \mathcal{R}_1 \rightarrow \mathcal{R}_2$ by $H_\Pi = h_2 h_1^{-1}$. H_Π is called the homography from $\mathcal{R}_1$ to $\mathcal{R}_2$ via the plane Π. By definition for every $M \in \Pi$, we have

$$H_\Pi \widetilde{m} = h_2 h_1^{-1}[P\ p]M = h_2 h_1^{-1} h_1 M = h_2 M = [P'\ p']M = \widetilde{m}'.$$

H_Π is represented by a 3×3 nonsingular matrix upto a scale and, hence, H_Π has eight independent parameters. Each image point contributes two parameters. Thus, given four image point correspondences of points in general position, the homography H_Π can be computed upto a scale [3], [21].

When $\Pi = \Pi_\infty$ (the plane at infinity) then $H_{\Pi_\infty} = H_\infty$. Then, $h_1 = P$ and $h_2 = P'$ and $H_\infty = h_2 h_1^{-1} = P'P^{-1}$. With our notations, we can prove the following: 1) $H_\Pi \widetilde{e} = \gamma \widetilde{e}'$ for some $\gamma \in \mathbb{R},\ \gamma \neq 0$, 2) $\widetilde{e}' = p' - H_\infty p$, and 3) $H_\infty \widetilde{e} = -\widetilde{e}'$ (See Appendix for proof).

We first develop a framework for the projective (relative affine) reconstruction of the components with respect to the same frame (Section 3). For this we define a projective reconstruction matrix which transforms the cameras into image computable form. Here, we follow broadly Luong and Vieville [12] for aligning the first camera $[P\ p]$ using relative affine framework. Define,

$$\mathcal{H} = \begin{bmatrix} P & p \\ L_N^t & \nu_N \end{bmatrix},\ L_N^t = -\nu_{\Pi_N}^t P,\ \ \nu_N = -\nu_{\Pi_N}^t p + \lambda_{e'}||e'||,$$

where $\nu_{\Pi_N}^t = e_N'^t (H_\Pi - H_\infty)$ and $e'_N = e'/||e'||$ (see Appendix for proof). It can be verified that $\mathcal{H}$ is invertible. Also the cameras can be transformed by $\mathcal{H}$, to

$$[P\ p] = [I_3\ 0]\mathcal{H},\ \ [P'\ p'] = [H_\Pi\ e'_N]\mathcal{H}.$$
$$\widetilde{m} = [P\ p]M = [I_3\ 0]\mathcal{H}M,\ \ \widetilde{m}' = [P'\ p']M = [H_\Pi\ e'_N]\mathcal{H}M.$$

Thus, the transformed cameras $[I_3\ 0]$ and $[H_\Pi\ e'_N]$ map $\mathcal{H}M$ to the same points as original cameras $[P\ p]$ and $[P'\ p']$ map M.

Next, using this reconstruction matrix, we propose a method of reconstruction of quadric components with respect to the same frame, based on the method of Shashua and Toelg [23]. In fact, the relative affine reconstruction has been necessitated by the quadric reconstruction. Values of invariants computed using these reconstructed components are used for recognition.

3 Projective Reconstruction of Translationally Repeated Objects

The main aim in this section is to develop a framework for the projective (relative affine) reconstruction of translationally repeated objects. The reconstruction problem for translationally repeated objects from a single image is best handled by converting the problem from the single image framework to the equivalent stereo image framework in [3]. If in the stereo conversion, the original camera is $[P\ p]$ and the translated camera is $[P'\ p']$, then we have $[P\ p]M' = [P\ p]TM = [P'\ p']M$. Therefore, we have $[P'\ p'] = [P\ p]T = [P\ P\mathbf{t} + p]$ giving $P' = P,\ p' = Pt + p$, and $COP_2 = \begin{pmatrix} -P^{-1}p - t \\ 1 \end{pmatrix}$. This shows that

$$T(COP_2) = COP_1. \tag{1}$$

Also, $H_\infty = P'P^{-1} = I$ and, hence, from Section 2.2, $H_\infty \widetilde{e} = \widetilde{e} = -\widetilde{e}'$.

We obtain a relative affine reconstruction on the lines of the fundamental work of Shashua and Navab [22]. The value of k computed in Lemma 3.1 characterizes the relative affine structure and has been obtained by Shashua and Navab [22] and Luong and Vieville [12]. By computing the k in Lemma 3.1, we will have reconstructed the first component pointwise. The second component is reconstructed with respect to the same frame in Theorem 3.2. The homography H_Π can be computed, in theory, using three noncollinear points on the plane Π [3]. But, all the scalar multiples of the homography are projectively the same homography. The proof of Lemma 3.1 [3], [21] and Theorem 3.2 takes into account the scaling at each stage, mathematically.

Lemma 3.1 Relative Affine Structure. *Let $M_i,\ i = 1, 2, 3, 4$ be four points in general position on the object S and let $M'_i,\ i = 1, 2, 3, 4$ be the corresponding points on the translated object S'. A single uncalibrated perspective image of an object containing S and S' together with the image point correspondences m_i and $m'_i,\ i = 1, 2, 3, 4$ of the above points is given. If $m = (x\, y\, 1)^t$ and $m' = (x'\, y'\, 1)^t$ is a point correspondence of a 3D point $M \in S$ and the corresponding translated point $M' \in S'$, then M is projectively reconstructed as $(x\, y\, 1\, k)^t$, where $k = \frac{(m' \times e'_N)^t (H_\Pi m \times m')}{||m' \times e'_N||^2}$. For proof see [3], [21].*

It is assumed that enough image information is given, so that the epipoles and the homography H_Π can be computed for a suitable plane Π using image information only [3], [21]. The actual scale of the homography is fixed using an additional point not lying on the plane. Having reconstructed the first component pointwise using Lemma 3.1, the second component is to be reconstructed with respect to the same frame. This is done in Theorem 3.2. This is not possible by a simple repeated application of the relative affine framework of Shashua and Navab [22], or by any other reconstruction framework, as the two components will be reconstructed with respect to different frames and, hence, cannot be used together for any meaningful computation like joint invariants. We have been able to incorporate and reconstruct both the components with respect to the same frame, which is a novel contribution of this paper.

Theorem 3.2. Projective Reconstruction: Translationally Repeated Objects. *Let $M_i,\ i = 1,2,3,4$ be four points in general position on the object S and let $M'_i,\ i = 1,2,3,4$ be the corresponding points on the translated object S'. A single uncalibrated perspective image of an object containing S and S' together with the image point correspondences m_i and $m'_i,\ i = 1,2,3,4$ of the above points is given. If $m = (x\ y\ 1)^t$ and $m' = (x'\ y'\ 1)^t$ is a point correspondence of a 3D point $M \in S$ and the corresponding translated point $M' \in S'$, then the translated point M' is projectively reconstructed as $(x'\ y'\ 1\ k')^t$, where*

$$k' = \frac{(m \times e'_N)^t[(H_\Pi m' - 2m') \times m]}{||m \times e'_N||^2}.$$

Here, $\Pi = < M_1, M_2, M_3 >$ = the plane defined by M_1, M_2, M_3.

Proof. Here, we will reconstruct M' projectively as $\mathcal{H}M'$.

$$\mathcal{H}M' = \mathcal{H}T(M) = \begin{pmatrix} P\widehat{M} + P\mathbf{t} + p \\ L_N^t\widehat{M} + L_N^t\mathbf{t} + \nu_N \end{pmatrix}.$$

Thus, $\mathcal{H}M' = \mathcal{H}M + \begin{pmatrix} P\mathbf{t} \\ L_N^t\mathbf{t} \end{pmatrix}$. So, we get $\mathcal{H}T(M) = \mathcal{H}M + \begin{pmatrix} P\mathbf{t} \\ L_N^t\mathbf{t} \end{pmatrix}$ for any 3D point M. In particular, when $M = COP_2$

$$\mathcal{H}T(COP_2) = \mathcal{H}(COP_2) + \begin{pmatrix} P\mathbf{t} \\ L_N^t\mathbf{t} \end{pmatrix}. \tag{2}$$

Premultiplying both sides of (2) by $[I_3\ 0]$ and simplifying using (1), we get

$$[P\ p](COP_1) = [P\ p](COP_2) + P\mathbf{t} \Rightarrow 0 = \widetilde{e} + P\mathbf{t},$$

i.e, $P\mathbf{t} = -\widetilde{e}$. Premultiplying by $[H_\Pi\ e'_N]$ in (2) and simplifying, we get

$$\begin{aligned}&[P'\ p'](COP_1) = [P'\ p'](COP_2) + H_\Pi P\mathbf{t} + e'_N L_N^t\mathbf{t} \\ &\Rightarrow \widetilde{e}' = -H_\Pi\widetilde{e} + e'_N L_N^t\mathbf{t},\end{aligned}$$

where $H_\Pi\widetilde{e} = \gamma\widetilde{e}'$. Thus, $L_N^t\mathbf{t} = (1+\gamma)\lambda_{e'}||e'||$.

Thus, we have

$$\mathcal{H}M' = \mathcal{H}M + \begin{pmatrix} -\widetilde{e} \\ (1+\gamma)\lambda_{e'}||e'|| \end{pmatrix}, \tag{3}$$

$$\begin{aligned}[I_3\ 0]\mathcal{H}M' = [I_3\ 0]\mathcal{H}M - \widetilde{e} \Rightarrow [P\ p]M' \\ = [P\ p]M - \widetilde{e} \Rightarrow \widetilde{m}' = \widetilde{m} - \widetilde{e}.\end{aligned} \tag{4}$$

From (3), we get

$$[H_\Pi\ e'_N]\mathcal{H}M' = [H_\Pi\ e'_N]\mathcal{H}M - H_\Pi\widetilde{e} + (1+\gamma)\lambda_{e'}||e'||e'_N$$

$$\begin{aligned}[P'\ p']M' &= [P'\ p']M - \gamma\widetilde{e}' + (1+\gamma)\lambda_{e'}||e'||\frac{e'}{||e'||} \\ &= \widetilde{m}' + \widetilde{e}' = \widetilde{m}' - \widetilde{e} = 2\widetilde{m}' - \widetilde{m}\end{aligned}$$

(using (4) and since $\widetilde{e}' = -\widetilde{e}$). But,

$$\begin{aligned}[P'\ p']M' = [H_\Pi\ e'_N]\mathcal{H}M' = [H_\Pi\ e'_N]\begin{pmatrix} \widetilde{m}' \\ \lambda' k' \end{pmatrix} \\ = H_\Pi\widetilde{m}' + \lambda' k' e'_N = \lambda'(H_\Pi m' + k' e'_N).\end{aligned}$$

Equating the two values, we get

$$2\widetilde{m}' - \widetilde{m} = \lambda'(H_\Pi m' + k' e'_N),$$

i.e., $-\lambda m = \lambda'(H_\Pi m' - 2m' + k' e'_N)$. Taking cross product with m and simplifying, we get

$$k' = \frac{(m \times e'_N)^t[(H_\Pi m' - 2m') \times m]}{||m \times e'_N||^2}$$

and

$$\mathcal{H}M' = (\widetilde{m'^t\ \lambda' k'})^t = \lambda'(m'^t\ k')^t \approx (m'^t\ k')^t = (x'\ y'\ 1\ k')^t,$$

as desired. □

We can now compute k', the relative affine structure, for each point on the repeated component and, hence, reconstruct each such point. Thus, the second component is completely reconstructed with respect to the same frame. As can be seen, in the expressions for k and k', all the entities are computable from the image. By (4), $\widetilde{m}' = \widetilde{m} - \widetilde{e}'$, which indicates a linear combination between $\widetilde{m}'$, $\widetilde{m}$, and $\widetilde{e}'$. Since we are using a single image, this implies that m, m', e' are collinear and this holds for all m, m'. Thus, e' can be computed by exploiting the fact that e' is the point of intersection of lines joining m_1, m'_1 and m_2, m'_2. Also, $H_\Pi m_i \cong m'_i,\ i = 1,2,3\ \ H_\Pi e \cong e'$, where $H_\Pi e = e'$ is used to set the scale. A procedure for computing H_Π and e'_N can be found in [3], [21].

Since H_Π computed above is upto a scale, therefore, a change in scale of H_Π will cause a change in the value of k and k'. In order to fix the scale of H_Π, compute k_4 for point M_4 not lying on the plane Π. Subsequently, use $\widehat{H}_\Pi = \frac{1}{k_4}H_\Pi$ as the homography matrix. The value of k now obtained is called the normalized value of k. The value of k and k' are obtained using the formulae in Lemma 3.1 and Theorem 3.2 (all values in the formulae are computable from the image).

4 Reconstruction of a Pair of Translationally Repeated Quadrics

This section deals with the objects considered in the previous section under the additional assumption that S is a quadric surface and $S' = T(S)$ is the translationally repeated quadric surface. The aim is to projectively reconstruct the quadric surfaces S and S' using the reconstruction carried out in Section 3, the main theoretical results for which are in Theorem 4.1 and 4.2. A computational procedure for the same is also given in this section. The importance of the study of such objects is obvious from the fact that quadrics appear in a repeated form, naturally in daily life in the form of minarets, dumbbells, paperweights, etc. Also, objects could be locally quadric as discussed in [6]. In this paper, we do reconstruction of repeated quadrics from a single image of the configuration which, to the best of our knowledge, has not been done before.

A *quadric surface* is an algebraic surface consisting of all points in $\mathbb{P}^3$ in homogeneous coordinates satisfying a homogeneous polynomial of degree 2 in four variables X_1, X_2, X_3, X_4 over the field $\mathbb{R}$ of real numbers. The general equation of the quadric surface is

$$S = S(X_1, X_2, X_3, X_4) = \Sigma_{i=1}^4\Sigma_{j=1}^4 q_{ij}X_iX_j = 0,$$

i.e., $S(X) = X^tQX = 0$, where $Q = (q_{ij})$ is a 4×4 real symmetric matrix and $X = (X_1\ X_2\ X_3\ X_4)^t$ is a homogeneous 4×1 vector. The quadric surface defined above is said to be proper if $\det(Q) \neq 0$, i.e., Q is nonsingular. The nonsingular 4×4 symmetric matrix Q upto a scale, completely determines a proper quadric surface and, as such, it is enough to determine Q. This contributes 10 parameters (as only the diagonal and upper diagonal entries are significant). Since the matrix Q and the nonzero scalar multiples of Q determine the same quadric surface, there are nine independent parameters. Thus, there exists a unique quadric surface passing through nine given points in general position in 3D. In general position means no four of these are coplanar. Each 3D point X (say) lying on the quadric contributes a single equation in the form $X^tQX = 0$. Since Q has nine unknowns, nine such equations are required. This indicates that we should have enough image information from which we can recover the nine parameters. This leads to the choice of image information for the reconstruction framework proposed in Theorem 4.2.

Given a 3D point not belonging to the quadric, tangents are drawn to the quadric from this point. If the given point is the COP of the perspective camera, the locus of the point of tangency is called the *rim* of the quadric and the image of the rim is called the *outline conic*. Since the tangency is preserved under a projective transformation and, as seen in the previous section, the images of a 3D point M by the original camera and the images of $\mathcal{H}M$ by the transformed camera are identical, the outline conic of the original quadric Q is the same as the outline conic of the reconstructed quadric $\widetilde{Q} = \mathcal{H}(Q) = \{\mathcal{H}M | M \in Q\}$.

Let

$$Q = \begin{pmatrix} Q_{33} & q \\ q^t & q_{44} \end{pmatrix},$$

Q_{33} a 3×3 matrix, q a 3×1 vector, q_{44} a scalar, be a quadric and let

$$\widetilde{Q} = \mathcal{H}(Q) = \begin{pmatrix} \widetilde{Q}_{33} & \widetilde{q} \\ \widetilde{q}^t & \widetilde{q_{44}} \end{pmatrix}$$

be the quadric to be reconstructed. It is not difficult to see that $\widetilde{Q} = (\mathcal{H}^{-1})^t Q \mathcal{H}^{-1}$ (upto a scale). In fact, $M = (X\ Y\ Z\ 1)^t$ lies on $Q \Leftrightarrow M^tQM = 0$. If $\widetilde{M}$ lies on $\widetilde{Q}$, $\widetilde{M}^t\widetilde{Q}\widetilde{M} = 0$. But, $M = \mathcal{H}^{-1}\widetilde{M}$ lies on Q, hence, $(\mathcal{H}^{-1}\widetilde{M})^tQ\mathcal{H}^{-1}\widetilde{M} = 0$ for every $M \in Q$. So, $\widetilde{M}^t(\mathcal{H}^{-1})^tQ\mathcal{H}^{-1}\widetilde{M} = 0$ and $\widetilde{Q} = (\mathcal{H}^{-1})^tQ\mathcal{H}^{-1}$ upto a scale. Now, we establish a relationship between the observed outline conic $\widetilde{C}$ and the reconstructed quadric $\widetilde{Q}$, which would help us in recovering the quadric parameters.

Lemma 4.1. Outline Conic of $\widetilde{Q}$. *The outline conic $\widetilde{C}$ of $\widetilde{Q}$ is determined by $\widetilde{C} = \widetilde{q}\widetilde{q}^t - \widetilde{q_{44}}\widetilde{Q_{33}}$.*

This has been proven in [23]. As an extension of this, we have also been able to show that $\det(Q) = -(\widetilde{q_{44}})^{-1}\det(\widetilde{C})$. Thus, $\widetilde{Q}$ is a proper quadric which implies $\widetilde{q_{44}} \neq 0$ and $\widetilde{C}$ is a proper conic.

Next in Theorem 4.2, we reconstruct $\widetilde{Q}$ and $\widetilde{Q}'$ from the given image information consisting of image point correspondences for the four points on Q and its translate Q' (points chosen are not on their rim) together with their outline conics, identified in a single uncalibrated perspective image. The four point correspondences are used to reconstruct four points on the components using the framework of Lemma 3.1 and Theorem 3.2. Thus, these provide four parameters in the form of the relative affine structure. That is, $k_i, i = 1, 2, 3, 4$ for the first component and $k'_i, i = 1, 2, 3, 4$ for the second component. The additional five parameters of the nine parameters required for a quadric are provided by the five parameters each of the outline conics. We use the method of Shashua and Toelg [23] to reconstruct the first quadric but, in order to reconstruct the repeated quadric, this theory needs to be modified, which is the main contribution of Theorem 4.2. Subsequently, in Theorem 4.3, we have shown that the scheme does not depend on the choice of the four points, which helps in generalizing the entire reconstruction-based recognition strategy.

Theorem 4.2. Reconstruction of $\widetilde{Q}$ and $\widetilde{Q}'$. *A single uncalibrated perspective image of a pair of proper quadrics Q and Q' is given where Q' is a translate of Q. Further image point correspondences of four distinguished noncoplanar points $M_i,\ i = 1, 2, 3, 4$ on Q and corresponding points $M'_i,\ i = 1, 2, 3, 4$ on Q' are given. Also, known in the image are corresponding outline conics. Then, the quadrics Q and Q' can be reconstructed projectively.*

Proof. Define the plane $\Pi = < M_1, M_2, M_3 >$. Let $m_i = (x_i\ y_i\ 1)^t$ and $m'_i = (x'_i\ y'_i\ 1)^t\ \ i = 1, 2, 3, 4$ be the corresponding image points of the distinguished points $M_i, M'_i,\ i = 1, 2, 3, 4$.

Reconstruction of $\widetilde{Q} = \mathcal{H}(Q)$. Let M be any point on Q having an image m. In Lemma 3.1, the reconstructed point $\mathcal{H}M \approx (x\ y\ 1\ k)^t$ has been computed. Since $\widetilde{Q} = \mathcal{H}Q$, we have by Lemma 4.1 $\widetilde{C} = \widetilde{q}\widetilde{q}^t - \widetilde{q_{44}}\widetilde{Q_{33}}$. As commented before, the given outline conic C of Q = the outline conic $\widetilde{C}$ of $\widetilde{Q}$. Also, $\widetilde{q_{44}} \neq 0$. Thus, $\widetilde{Q_{33}} = \frac{\widetilde{q}\widetilde{q}^t - \widetilde{C}}{\widetilde{q_{44}}} = \frac{\widetilde{q}\widetilde{q}^t - C}{\widetilde{q_{44}}}$ and

$$\widetilde{Q} = \begin{pmatrix} \widetilde{Q_{33}} & \widetilde{q} \\ \widetilde{q}^t & \widetilde{q_{44}} \end{pmatrix},$$

is known if we can compute $\widetilde{q}$ and $\widetilde{q_{44}}$ consisting of three unknowns from $\widetilde{q}$ and 1 from $\widetilde{q_{44}}$. We have $(m^t\ k)\widetilde{Q}(m^t\ k)^t = (x\ y\ 1\ k)\widetilde{Q}(x\ y\ 1\ k)^t = 0$, which, after simplification, gives the equation $(m^t\widetilde{q} + k\widetilde{q_{44}})^2 = m^tCm$. This gives

$$m^t\widetilde{q} + k\widetilde{q_{44}} = \pm\sqrt{m^tCm}. \tag{5}$$

The sign of the right hand side can be chosen unambiguously to be positive (see Remark 4.3 given after the proof). Now, $\widetilde{q}$ and $\widetilde{q_{44}}$ can be computed by solving set of four equations obtained from (5) by substituting $m = m_i = (x_i\ y_i\ 1)^t$ and k_i as computed in Lemma 3.1, $i = 1, 2, 3, 4$. Thus, $\widetilde{Q}$ has been reconstructed.

Similarly, we can reconstruct $\widetilde{Q}' = \mathcal{H}(Q')$ using $m'_i = (x'_i\ y'_i\ 1)^t$ and k'_i as computed in Theorem 3.2, $i = 1, 2, 3, 4$ and the knowledge of the outline conic C' of Q'. □

Remark 4.3. The two signs in (5) would give two values of k, i.e., k_1 and k_2. The two points $(x\ y\ 1\ k_1)^t$ and $(x\ y\ 1\ k_2)^t$

are the two points of intersection of the ray $< \mathcal{HO}\ \mathcal{HM} >$ with the quadric $\widetilde{Q}$, where $m = (x\ y\ 1)^t \approx [P\ p]M$. The problem is to pick k unambiguously so as to choose the unoccluded point, which in our case would be the one closer to the transformed $COP_1 = \mathcal{HO} \approx (0\ 0\ 0\ 1)^t$. By referring to closeness, we are not trying to define the distance between $\mathcal{HM}$ and $\mathcal{HO}$ since these are projective points and the concept of distance is not defined between them. Each transformed 3D point is equivalent to $(x\ y\ 1\ k)^t$, thus, we have been able to associate a number k with each 3D point of the ray $< \mathcal{HO}\ \mathcal{HM} >$. The relative affine structure k can be expressed as $k = \frac{d}{z}\frac{z_4}{d_4}$, where d, d_4 are perpendicular distances of M and M_4 (point lying outside the plane Π), respectively, from the plane Π and z, z_4 are the depths of these points from the origin [21]. M_4 is the point lying outside the plane Π formed by the points M_1, M_2, M_3. It is the point used to fix the scale of H_Π and to normalize k. The choice between k_1 and k_2 is made depending on the position of M_4 with respect to the COP and Π. If M_4 lies between COP and Π, $k = max(k_1, k_2)$ and if M_4 and COP are on opposite sides of Π, then $k = min(k_1, k_2)$. We can assume without loss of generality that $\tilde{q}_{44} > 0$, thus, k takes the maximum value when $\sqrt{m^t C m}$ is assigned positive sign. By adjusting the scale of H_Π, it can be shown that all the points on the ray $< \mathcal{HO}\ \mathcal{HM} >$ are such that the value of k decreases as we move away from the origin, with $k = 0$ on the plane Π and the point with maximum k is the one closest to the origin. Thus, the first point on the quadric which $< \mathcal{HO}\ \mathcal{HM} >$ meets is the one with maximum k. Therefore, it can be inferred that a positive sign should be assigned to $\sqrt{m^t C m}$ in the (5). Hence, the choice of k has been made unambiguous.

Next, we give the computational scheme for quadric reconstruction. The algorithm for the reconstruction of a virtual quadric surface, using two images of the quadric, has been given by Shashua and Toelg [23]. We have used that algorithm to compute the first quadric and then used the result of Theorem 4.2, to compute the repeated quadric with respect to the same frame.

Algorithm: Reconstruction of Translationally Repeated Quadrics

Input: The outline conics C_1 and C_2 of the two translated quadrics, images m_1, m_2, m_3, m_4 of four distinguished points on the quadrics and their correspondences m_1', m_2', m_3', m_4'.

Output: Matrices of the translationally repeated reconstructed quadrics $\widetilde{Q}_1$ and $\widetilde{Q}_2$.

Stepwise Methodology:

1. Pick points on the outline conic C_1 detected in the image and fit a conic to it using Bookstein's algorithm. Repeat the same for C_2.
2. Choose $k_1 = 0, k_2 = 0, k_3 = 0$, and $k_4 = 1$ to obtain points $(x_1\ y_1\ 1\ 0)^t$, $(x_2\ y_2\ 1\ 0)^t$, $(x_3\ y_3\ 1\ 0)^t$, and $(x_4\ y_4\ 1\ 1)^t$.
3. Solve for $\widetilde{q}_{44}^1$ and $\widetilde{q}^1$ using the equations
$$\begin{pmatrix} x_1 & y_1 & 1 & 0 \\ x_2 & y_2 & 1 & 0 \\ x_3 & y_3 & 1 & 0 \\ x_4 & y_4 & 1 & 1 \end{pmatrix} \begin{pmatrix} \widetilde{q}_1^1 \\ \widetilde{q}_2^1 \\ \widetilde{q}_3^1 \\ \widetilde{q}_{44}^1 \end{pmatrix} = \begin{pmatrix} \sqrt{m_1^t C_1 m_1} \\ \sqrt{m_2^t C_1 m_2} \\ \sqrt{m_3^t C_1 m_3} \\ \sqrt{m_4^t C_1 m_4} \end{pmatrix}$$
to compute $\widetilde{Q}_1$.
4. Compute k_1', k_2', k_3', k_4' using formula in Theorem 3.2 and obtain the reconstructed points $(x_i'\ y_i'\ 1\ k_i')^t$, $i = 1, 2, 3, 4$.
5. Solve for $\widetilde{q}_{44}^2$ and $\widetilde{q}^2$ using the equations
$$\begin{pmatrix} x_1' & y_1' & 1 & k_1' \\ x_2' & y_2' & 1 & k_2' \\ x_3' & y_3' & 1 & k_3' \\ x_4' & y_4' & 1 & k_4' \end{pmatrix} \begin{pmatrix} \widetilde{q}_1^2 \\ \widetilde{q}_2^2 \\ \widetilde{q}_3^2 \\ \widetilde{q}_{44}^2 \end{pmatrix} = \begin{pmatrix} \sqrt{m_1^t C_2 m_1} \\ \sqrt{m_2^t C_2 m_2} \\ \sqrt{m_3^t C_2 m_3} \\ \sqrt{m_4^t C_2 m_4} \end{pmatrix}$$
to compute $\widetilde{Q}_2$.

As can be seen, the choice of four point correspondences of points in general position, is essential for reconstruction. Therefore, it becomes important to discuss how critical the choice of four points is to the recognition strategy. A greater independence in the choice of these points will lead to a more general recognition strategy. In Theorem 4.3, we discuss the effect of changing these points on the reconstructed quadrics.

Theorem 4.3. *Let Q be a quadric and Q' its translate. M_1, M_2, M_3, M_4 are the four distinguished points on Q and M_1', M_2', M_3', M_4' are their correspondences on the quadric Q'. The reconstructed quadrics are $\widetilde{Q}$ and $\widetilde{Q}'$, respectively. By changing the distinguished points to $\bar{M}_1, \bar{M}_2, \bar{M}_3, \bar{M}_4$, the reconstructed quadrics are $\widetilde{\bar{Q}}$ and $\widetilde{\bar{Q}}'$, respectively. These are projectively equivalent to the original pair, that is, there exists a projective transformation $\widehat{\mathcal{H}}$ such that $\widetilde{\bar{Q}} = \widehat{\mathcal{H}}^t \widetilde{Q} \widehat{\mathcal{H}}$ and $\widetilde{\bar{Q}}' = \widehat{\mathcal{H}}^t \widetilde{Q}' \widehat{\mathcal{H}}$. (See [4] for proof).*

Thus, an alternate choice of four points leads to a projectively equivalent reconstruction of the components. Since we use these components to compute the joint projective invariants, and the values of the invariants remain the same for projectively equivalent configurations, any four points in general position can be used for reconstructing projectively equivalent quadrics. This makes the reconstruction scheme independent of the choice of these four points, upto a projective transformation. This in turn generalizes the recognition strategy.

Having reconstructed the quadrics, we will use these to compute projective invariants, the values of which will be used for recognition. The invariants are computed in the next section. The reconstructed quadrics are proper because the outline conics were nondegenerate and, hence, by remark following Lemma 4.1, the reconstructed quadrics are proper. Also, by Theorem 4.3, the choice of distinguished points is not crucial to the strategy.

5 Recognition of Quadric Configurations

In this paper, we propose an invariance-based recognition strategy for repeated quadric configurations, where the

invariants are computed using the reconstructed components. By a quadric configuration, we mean a configuration consisting of a pair of translationally repeated quadrics which are rigidly connected. In the previous section, we have reconstructed upto a projective transformation, a pair of translationally repeated proper quadrics, using the image information only. The reconstruction process yields reconstructed quadrics which are not projectively equivalent if the same pair is separated by different translations. In this section, we compute the joint projective invariants of a pair of proper quadrics for the purpose of recognition of quadric configurations. It may be said at the very outset that the invariants computed here hold for any pair of proper quadrics, irrespective of whether they are repeated or not. The nature of the invariants is such that the repeated quadrics with different translations as well as different nature of quadrics, will be recognized as different configurations. It is important that the reconstruction of both these quadrics is with respect to the same frame (as in our reconstruction framework) since otherwise, having obtained quadrics in different frames, it would not have been possible for us to compute their joint invariants. In the following, we present a scheme for computing the **joint projective invariants of a pair of proper quadrics**:

Let Q_1 and Q_2 be a pair of proper quadrics defined upto a scale by 4×4 nonsingular symmetric matrices A and B, respectively. Let $T \in PGL_4(\mathbb{R})$ be any projective transformation. Define transformed quadrics as $\overline{Q}_1 = T(Q_1) = \{TM | M = (X\ Y\ Z\ 1)^t \in Q_1\} = \{TM | M^t A M = 0\}$ and $\overline{Q}_2 = T(Q_2) = \{TM | M^t B M = 0\}$. Then, it can be shown that, $\det(\overline{A}) = |\overline{A}| = |T^{-1}|^2 |A|$ and $\det(\overline{B}) = |\overline{B}| = |T^{-1}|^2 |B|$ [3], [5].

To compute the number of projective invariants of the configuration space consisting of a pair of quadrics Q_1 and Q_2, we use the well-known formula (Gros and Quan [9]):

$$\begin{aligned} &\textit{Number of independent invariants} \\ &= \textit{Dimension of the configuration space} \\ &\quad - \textit{Dimension of the transformation group.} \end{aligned}$$

Since each quadric contributes nine independent parameters, hence, the dimension of the configuration space consisting of a pair of quadrics is $9 + 9 = 18$. Now, the projective group, $PGL_4(\mathbb{R})$, which is the multiplicative group of all 4×4 nonsingular matrices upto a scale, has 15 degrees of freedom. So from the formula there are $18 - 15 = 3$ independent invariants.

Now, Q_1 and Q_2 are determined by matrices A and B upto a scale, so, if the projective invariants are computed with the help of matrices A and B, then these should be independent of all scalars $\alpha, \beta \neq 0$ and all $T \in PGL_4(\mathbb{R})$ when computed from $\alpha A,\ \beta B,\ (T^{-1})^t A T^{-1}, (T^{-1})^t B T^{-1}$. In the next theorem, we overcome these difficulties and compute a set of three projective invariants. The same methodology can be used to obtain other sets of independent invariants.

Theorem 5.1. (Projective Invariants). *If Q_1 and Q_2 are the two proper quadrics defined by symmetric nonsingular matrices A and B, respectively, upto a scale, then $\{\frac{I_3^2}{I_1 I_5}, \frac{I_2 I_4}{I_1 I_5}, \frac{I_4^2}{I_3 I_5}\}$ defines a desired set of joint projective invariants, where $I_k,\ k = 1, 2, 3, 4, 5$ are defined by*

$$|\lambda A + \mu B| = \lambda^4 I_1 + \lambda^3 \mu I_2 + \lambda^2 \mu^2 I_3 + \lambda \mu^3 I_4 + \mu^4 I_5.$$

As a consequence, we have $I_1 = |A|$, $I_5 = |B|$, $I_2 = \Sigma_{i=1}^4 b_{ij} A_{ij}$, A_{ij} is the cofactor of a_{ij} in $|A|$, $I_4 = \Sigma_{i=1}^4 a_{ij} B_{ij}$, B_{ij} is the cofactor of b_{ij} in $|B|$, and I_3 = the sum of six determinants of order 4 in which any two columns are from A and any other two columns are from B. (See [3], [4] for proof).

Theorem 5.1 gives one set of joint projective invariants. Alternate choices are also possible, for example $\{\frac{I_2 I_3}{I_1 I_5}, \frac{I_3 I_4}{I_2 I_5}, \frac{I_2 I_4}{I_1 I_5}\}$. As can be seen, each of the $I_k, k = 1, \cdots, 5$ are computable from the matrix of the quadrics. From the given image information of translationally repeated quadrics Q and Q', in Section 5, we have projectively reconstructed $\widetilde{Q} = \mathcal{H}(Q)$ and $\widetilde{Q}' = \mathcal{H}(Q')$ upto a suitable $\mathcal{H} \in PGL_4(\mathbb{R})$. Thus, using the matrices of the quadrics, a set of projective invariants for the pair of quadrics $\widetilde{Q}$ and $\widetilde{Q}'$ can be computed using Theorem 5.1 above. These will be the same if we compute from the original pair of quadrics Q and Q' as these are projectively equivalent to the reconstructed quadrics. We now have the desired invariants for the purpose of recognition of quadric configurations. Since changing the four point correspondences just leads to the reconstruction of a pair of projectively equivalent quadrics (Theorem 4.3), the choice of these four points in the reconstruction process, has no effect on the value of the proposed projective invariants. Hence, the choice of these points is not crucial to the recognition strategy, making it general in application.

6 Recognition Experiments

The experiments were undertaken in order to study the applicability of this invariant-based recognition strategy to the recognition problem.The two major aspects of applicability are the discriminatory power and the stability of the strategy which are investigated via experiments. Initially, we experimented on synthetic data in order to verify the theory [3]. The recognition strategy is then applied to experimental scenes (Figs. 2, 3, 4, and 5) and images of real life 3D objects with translationally repeated quadric components like images of monuments with multidome architecture (Figs. 6, 7, and 8). Results of these experiments establish the effectiveness of our reconstruction-based recognition scheme.

For all images, the conics were fitted interactively by using Bookstein's algorithm [1] (Fig. 1). The correspondences between known points on the translationally repeated objects were used and have been distinctly identified in some objects to establish correspondence. The processing routines were developed using MATLAB.

6.1 Discriminatory Power of Invariants

In order to compare two sets of values of invariants, a distance measure is required. For all pairs of different images im_i, im_j, we define the distance used by Quan and Veillon in [18], as

$$\Sigma_{k=1}^3 (V_k[im_i] - V_k[im_j])^2, \tag{6}$$

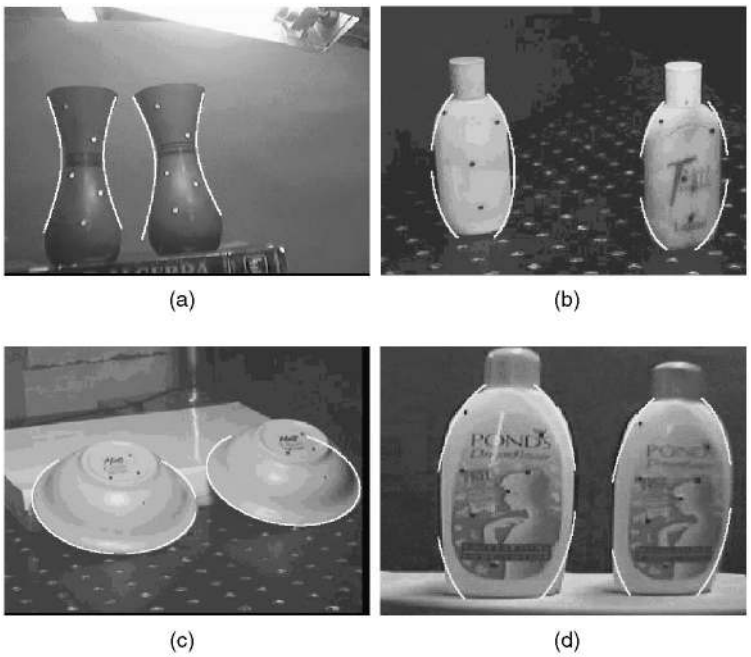

Fig. 1. Outline conics fitted to some experimental scenes.

where $V_k[im_i]$ is the value of the kth invariant of image i. For our results, we will take the linearly independent set to be $\{\frac{I_3^2}{I_1 I_5}, \frac{I_2 I_4}{I_1 I_5}, \frac{I_4^2}{I_3 I_5}\}$.

6.1.1 Experimental Scenes

We take the experimental scenes (Figs. 2, 3, 4, and 5). Each of the vases (Fig. 2) are modeled as hyperboloids, bowls (Fig. 3) and bottles (Figs. 4 and 5) as ellipsoids. We apply our framework to each of the images and compute three independent invariants which are shown in Table 1. The distances between the sets of invariant values of the images are shown in Table 2. The actual distances obtained using (6) have been relatively scaled by a factor of 10^{13} so that they can be meaningfully analyzed.

It can be observed that the distances indicate the discriminatory power of the invariants. Two views of the same pair of vases are projectively equivalent. This scenario is equivalent to the camera being fixed and the same projective transformation being applied to quadrics. The study of the distances in Table 2 show that the

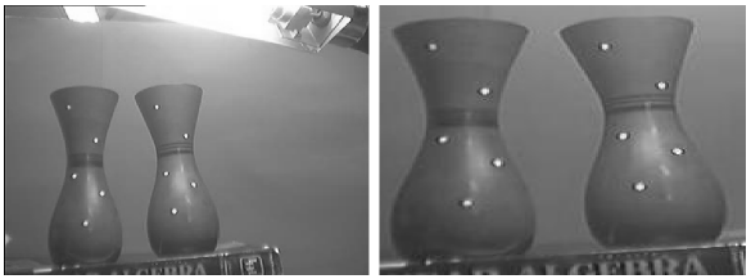

Fig. 2. Two views of transitionally repeated vases.

Fig. 3. Two views of transitionally repeated bowls.

Fig. 4. Two views of transitionally repeated bottles.

Fig. 5. (a), (b) Two views of transitionally repeated. (c) Bottles seperated by a different translation.

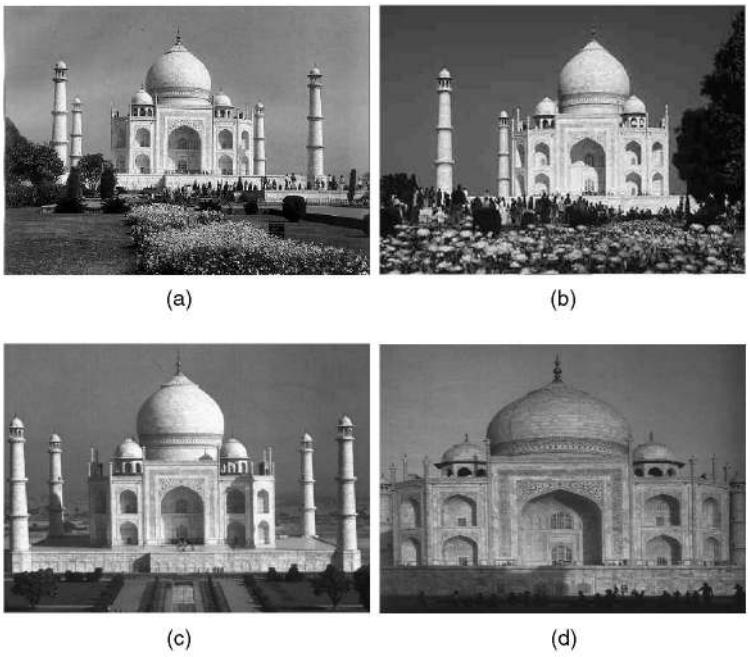

Fig. 6. Views of the Taj Mahal, Agra, India.

distance between projectively equivalent configurations (say, Figs. 3a and 3b) is much less as compared to its distance from other configurations (say, Figs. 4, 5, and 6), which are not projectively equivalent to it. This indicates that our recognition strategy, in which invariants are computed using reconstructed components, has a high discriminatory power.

The invariants also have the capability of distinguishing between the configurations on the basis of translation between them. Figs. 5a and 5b are two views of the same configuration, that is, the components have the same translation and Fig. 5c has a different translation. This is indicated by the fact that the distance between Figs. 5a and 5b is 4.5975 which is less than the distance between Figs. 5a and 5c (2.754e6) and Figs. 5b and 5c (2.747e6).

It has also been tested that the discriminatory power of the invariants still hold when a different set of independent invariants is chosen, e.g., $\{\frac{I_1 I_5}{I_3^2}, \frac{I_1 I_5}{I_2 I_4}, \frac{I_2^2}{I_1 I_3}\}$. The values of these invariants for the experimental scenes and the distances between the invariants are given in [3]. The distances have also been computed using a set of invariants as those in Table 2, but the first two invariants have been inversed [3].

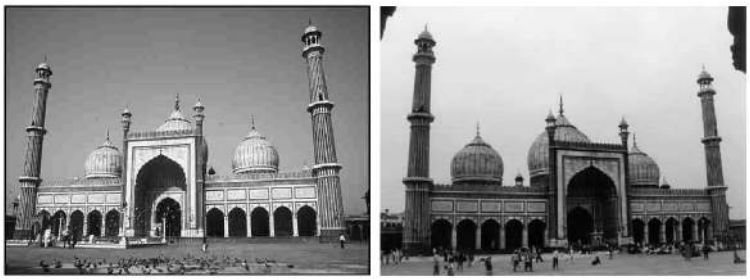

(a) (b)

Fig. 7. Views of the Jama Masjid, Delhi, India.

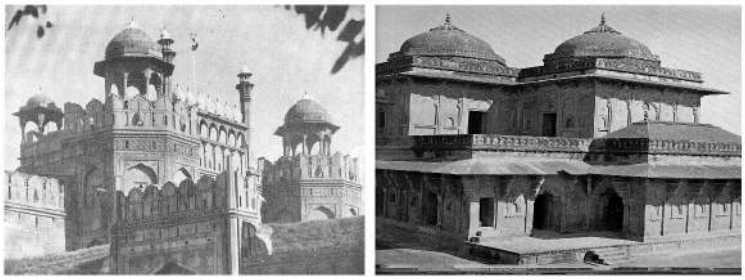

(a) (b)

Fig. 8. Views of the (a) Red Fort, Delhi and (b) Birbal's Tomb, Agra.

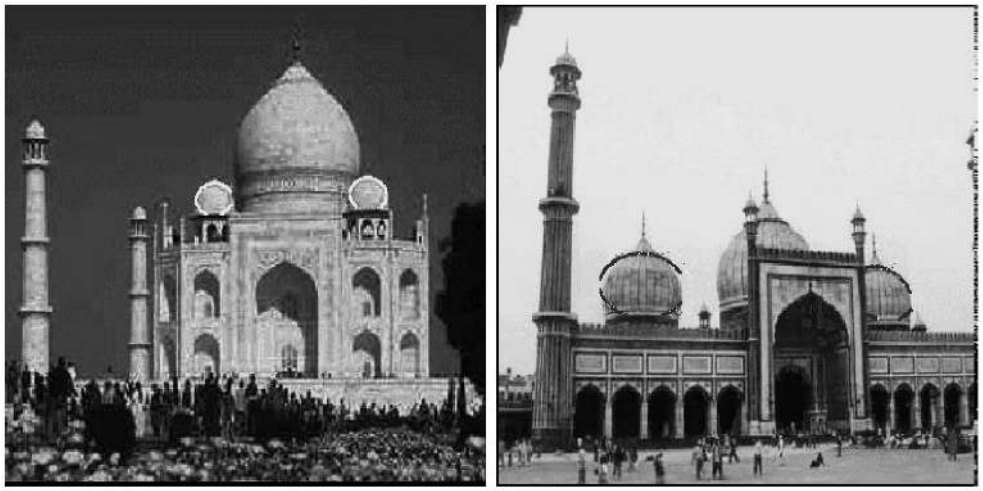

(a) (b)

Fig. 9. Conics fitted to repeated domes of monuments.

Inspite of the values of the first two invariants being very small compared to the third, the distances are able to distinguish the configurations.

6.2 Application

As an application, the experiments are carried out on images of monuments with multidome architecture. The aim is to be able to extract features which are similar between images of the same monument. This application indicates the applicability of the approach to content-based image retrieval.

Our framework is applied to monuments in Figs. 6, 7, and 8, which have minarets and domes which are translationally repeated. These monuments can be characterized by the repeated domes. Each of these domes can be modeled as a quadric. Due to the distance from which the photograph has to be taken in order to get the two domes in view, the projective distortion is not too much. As a result, the outline conics seen in the image do not vary much, which aid in recognition. Occlusion is not a major issue because the size of the structures makes it difficult for one of the domes to be completely covered. Also, these monuments have parapets around the domes, or engravings on the dome, which can aid in the choice of distinguished points. The perfect symmetry of these domes allow a wide range of views to be acceptable.

In each of the images of the monuments, the outline conic was fitted to the domes. The fitted outline conics for two of the monuments is shown in Fig. 9. The four points chosen were two corners of the parapet, one point just below the steeple, and the fourth point as the centre of the fitted conic. As is evident from the choices, these points are

TABLE 1
Values of Invariants of Experimental Scenes

Fig. No.	$\frac{I_3^2}{I_1 I_5}$	$\frac{I_2 I_4}{I_1 I_5}$	$\frac{I_4^2}{I_3 I_5}$
2 (a)	4.9724e6	1.2101e6	-1.3466e3
2 (b)	8.8897e6	2.5712e6	-1.4952e3
3 (a)	3.927e5	-1.6973	-2.1646e4
3 (b)	4.4671e5	-6.2543e5	-2.4266e4
4 (a)	5.6329e7	1.3681e7	-7.2899e3
4 (b)	6.3996e7	1.5734e7	-7.2382e3
5 (a)	9.1642e7	2.2680e7	-3.1159e4
5 (b)	9.8416e7	2.2992e7	-3.3064e4
5 (c)	5.2821e9	7.999e8	-1.1556e4

always found on the domes in question. A quadric was reconstructed with respect to each dome, and the invariants were computed with each pair. This was first done for four images of the Taj Mahal, (Fig. 6), then two images of the Jama Masjid (Fig. 7), and one each of the Red Fort (Fig. 8a) and Birbal's house (Fig. 8b). The distances between these invariants are shown in Table 3. Here, also the distances have been relatively scaled in order to make their analysis meaningful.

The values in Table 3 show that the distance between invariants for Figs. 6a, 6b, 6c, and 6d are of the order 10^0. The distances of these from the invariants of Figs. 7a and 7b and Figs. 8a and 8b are of the order 10^3. Similarly, distances between the invariants for the two images Figs. 7b and 7a is 0.2075, and the distances of Fig. 7b from Figs. 8a and 8b are 1.1969 and 1.243, respectively.

These distance values indicate the discriminatory ability of the strategy with respect to features obtained from the monuments. Hence, this invariant-based recognition strategy can be used for indexing images of these type of monuments.

6.3 Stability of the Invariant-Based Recognition Strategy

The stability of the recognition strategy implicitly takes into account the stability of the reconstruction scheme and the stability of the invariants computed using the reconstructed quadrics. It brings to fore two main issues:

- The ability of the strategy to handle the effect of perturbation in the correspondences between translated points and use of an alternate set of correspondences for reconstruction.
- The ability of the strategy to discriminate and cluster images of a configuration taken from different views. A Principal Component Analysis-based feature extraction and classification scheme has been used for studying this aspect of stability.

We now analyze both these issues in detail.

6.3.1 Stability: Correspondence Related Issues

We study the effect of perturbation in the correspondences via a simulated experiment. We take a pair of quadrics and their images, the outline conics. We perturb the position of the corresponding points on the translated quadric, keeping the points on the first quadric the same. The entire reconstruction strategy is now applied to it and we compute the invariants shown in Table 4. We find the distance between the values obtained without perturbing the points

TABLE 2
Distances (Scaled by 10^{13}) between Objects in Terms of Invariants Values

Fig. No.	2 (a)	2 (b)	3 (a)	3 (b)	4 (a)	4 (b)	5 (a)	5 (b)	5 (c)
2 (a)	0	1.7198	2.2878	2.3852	279.2983	369.4722	797.2611	920.6053	2.8486e6
2 (b)	1.7198	0	7.9712	8.1503	237.3878	320.9959	725.2342	843.1870	2.8442e6
3 (a)	2.2878	7.9712	0	0.0211	332.0669	429.8302	884.8581	1.0145e3	2.8536e6
3 (b)	2.3852	8.1503	0.0211	0	332.7461	430.6137	385.9759	1.0156e3	2.8536e6
4 (a)	279.2983	237.3878	332.0669	332.7461	0	6.3003	132.8032	185.7998	2.7926e6
4 (b)	369.4722	320.9959	429.8302	430.6137	6.3003	0	81.2563	127.7382	2.7843e6
5 (a)	797.2611	725.2342	884.8581	385.9759	132.8032	81.2563	0	4.5975	2.7545e6
5 (b)	920.6053	843.1870	1.0145e3	1.0156e3	185.7998	127.7382	4.5975	0	2.7474e6
5 (c)	2.8486e6	2.8442e6	2.8536e6	2.8536e6	2.792e6	2.7843e6	2.7545e6	2.7474e6	0

TABLE 3
Distances (Scaled by 10^{17}) between Invariants of Monuments

Fig. No.	6 (a)	6 (b)	6 (c)	6 (d)	7 (a)	7 (b)	8 (a)	8 (b)
6 (a)	0	9.8278	2.0833	6.6732	275.7703	260.8493	297.1625	297.8935
6 (b)	9.8728	0	3.0299	6.1735	186.9058	174.7020	204.3098	204.9123
6 (c)	2.0833	3.0299	0	2.9869	230.3271	216.7116	249.8673	250.5372
6 (d)	6.6732	6.1735	2.9869	0	209.5282	196.5934	228.47	229.1075
7 (a)	275.7703	186.9058	230.3271	209.5282	0	0.2075	0.4127	0.4403
7 (b)	260.8493	174.7020	216.7116	196.5934	0.2075	0	1.1969	1.2437
8 (a)	297.1625	204.3098	249.8673	228.47	0.4127	1.1969	0	4.5045e-4
8 (b)	297.8935	204.9123	250.5372	229.1075	0.4403	1.2437	4.5045e-4	0

TABLE 4
Values of Invariants Computed by Introducing Perturbation in the Points on the Translated Quadratic and Their Distance from the Invariants of the Unperturbed Configuration

Perturbation.	$\frac{I_3^2}{I_1 I_5}$	$\frac{I_2 I_4}{I_1 I_5}$	$\frac{I_4^2}{I_3 I_5}$	Distance
0	4423384.23	1058179.07	-1853.90	0
-3.77	1373846.98	289399.62	-1045.86	0.31
-1.41	2033349.98	472029.21	-1473.96	0.25
1.77	2118580.38	493546.10	-1437.05	0.24
0.33	2042958.21	472760.08	-1529.48	0.25
0.62	2671527.37	618490.52	-1457.79	0.18
1.27	2073973.62	482700.82	-1445.02	0.24
-0.89	2122799.81	494555.49	-1436.63	0.24
0.14	2072807.91	482411.47	-1445.36	0.24
1.84	1175540.12	263559.01	-1122.90	0.33
-0.28	1441219.56	327752.67	-1218.26	0.31
2.21	5722208.35	1273118.05	-1602.69	0.13
-2.68	1186659.72	8802.28	-1421.13	0.34
4.03	55816180.55	-4292103.83	-127012.01	5.17
6.71	2745352172.27	-52261095.58	-447094.31	274.14
3.88	48261562.80	297179.62	-876.32	4.38
5.87	1254875645.96	-184642525.59	-1662503.11	126.42

The distances have been scaled by 10^7 so that they can be analyzed relatively. The values have been rounded to two places after the decimal.

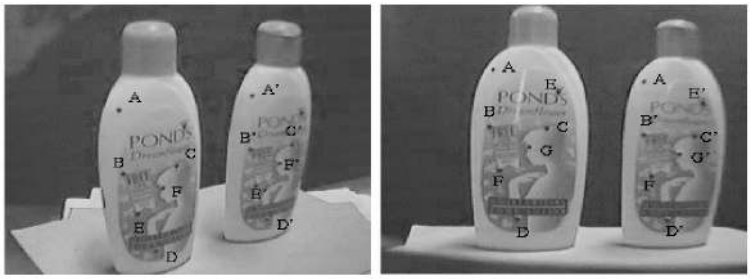

Fig. 10. Configurations with marked points for picking correspondences.

and those obtained by perturbing the points. The distances have been scaled by the order of 10^7 to make the relative comparison of distances meaningful. It can be seen that small perturbations of two-three pixels can be handled, that is, the distances from the unperturbed case is small. But, the distance increases with the increase in displacement of the pixels. This is realistic because a perturbation of five or more pixels may cause the point to lie outside the outline conic. Thus, the invariant values have been found to be stable for small perturbations in points.

Also, it has been proved in Theorem 4.3 that the choice of point correspondences is not crucial to the reconstruction-based recognition strategy. We have experimentally verified this for the scenes in Fig. 10 by taking different sets of distinguished points. The values of the invariants are shown in Table 5. Values have been found to be similar. This indicates the stability of the quadric reconstruction and the experimental validation that any four points in general position can be chosen.

6.3.2 Principal Component Analysis

Use of trainable classifiers provide a mechanism to decide upon class boundaries depending upon variations of the invariant value over an example set [19]. Hence, we have used principal component analysis for feature extraction, so that class separability is maximized.

For principal component analysis, we take three configurations each containing a pair of translationally repeated quadrics (Figs. 11a, 11b, 11c, and 11d, 12a, 12b, 12c, and 12d, 13a, 13b, 13c, and 13d). For each of these, we reconstruct the pair of quadrics as explained in Section 4 and compute the values of seven invariants

$$\{\frac{I_1 I_5}{I_3^2}, \frac{I_2 I_4}{I_3^2}, \frac{I_2 I_5}{I_3 I_4}, \frac{I_1 I_5}{I_2 I_4}, \frac{I_3 I_5}{I_4^2}, \frac{I_1 I_4}{I_2 I_3}, \frac{I_1 I_3}{I_2^2}\}$$

for each of the images. These values form the vector of invariants for each image. We do an eigenspace analysis of these invariant vectors. We compute the covariance matrix C of these vectors, the eigen values of the covariance matrix, and their corresponding eigen vectors. The eigen values are {1.9822e-13, 2.5216e-12, 2.8992e-9, 8.2652e-7, 2.5028e-5, 7.6463e-4, 0.0098}. Then, we obtain the projection of the invariant vectors on to the space defined by the eigen vectors corresponding to the three largest eigen values (as a pair of quadrics has three independent invariants). We can categorize these images (Figs. 11, 12, and 13) into three classes on the basis of their projective equivalence:

- Class I: Figs. 11a, 11b, 11c, and 11d,
- Class II: Figs. 12a, 12b, 12c, and 12d,
- Class III: Figs. 13a, 13b, 13c, and 13d.

TABLE 5
Effect of Change in Distinguished Points on the Invariants

Fig. No.	Distinguished points	$\frac{I_1 I_5}{I_3^2}$	$\frac{I_1 I_5}{I_2 I_4}$	$\frac{I_4^2}{I_3 I_5}$
10 (a)	A, B, C, D	2.4716e-8	1.0025e-7	-1.7372e4
	A, E, C, D	3.1075e-9	1.2624e-8	-1.4107e4
	A, E, F, D	1.0617e-8	4.3838e-8	-1.0216e4
	A, B, F, D	2.3925e-8	9.7016e-8	-8.3501e3
10 (b)	A, B, C, D	4.952e-8	1.9942e-7	-1.1122e4
	E, F, G, H	1.6836e-8	6.8391e-7	-9.9156e3

Their separation is characterized using the Mahalanobis distance

$$D(Y_i, Class_j) = (Y_i - \overline{Y}_j)^t C_j^{-1} (Y_i - \overline{Y}_j), \quad (7)$$

where C_j is the covariance matrix of class j and $D(Y_i, Class_j)$ denotes the distance of vector Y_i from the jth class. The Mahalanobis distance of the projected vectors corresponding to the experimental scenes, from the three identified classes are shown in Table 6, which indicate that the classes are well separated.

We now consider two novel views (Figs. 14a and 14b) of Fig. 12 and Fig. 13, respectively. The Mahalanobis distance of these projected vectors of these images from the three classes are given in Table 6. The distances from the classes correctly classify the image Fig. 14a as belonging to Class II and Fig. 14b to be that of the configuration corresponding to Class III. The distance of the invariants computed for the quadrics reconstructed using different sets of four points, shown in Fig. 10b, on the projected feature space, from the three classes, show (Table 6) that they have been correctly classified as Class II.

The results establish that the invariants computed via the reconstruction-based recognition strategy are such that we are able to categorize these images correctly into classes, despite variations in viewpoint, which is equivalent to applying the same projective transformation to both the quadrics keeping the camera fixed. They are also stable to change in the set of point correspondences and perturbation in points.

7 Conclusions and Future Work

In this paper, we have given a scheme for invariant-based recognition for translationally repeated quadric configurations via a reconstruction framework. A mathematical framework for the reconstruction of translationally repeated objects, in general, and translationally repeated quadrics in

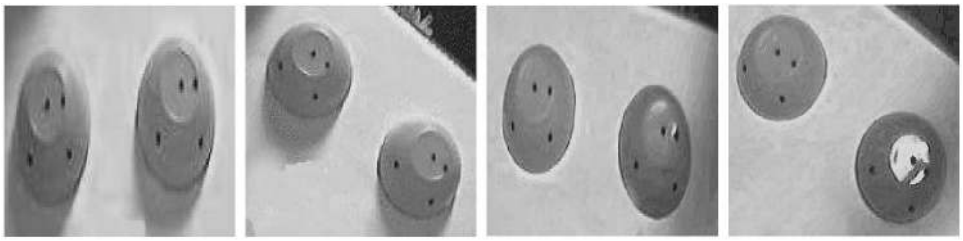

Fig. 11. View of Scene 1 for stability analysis.

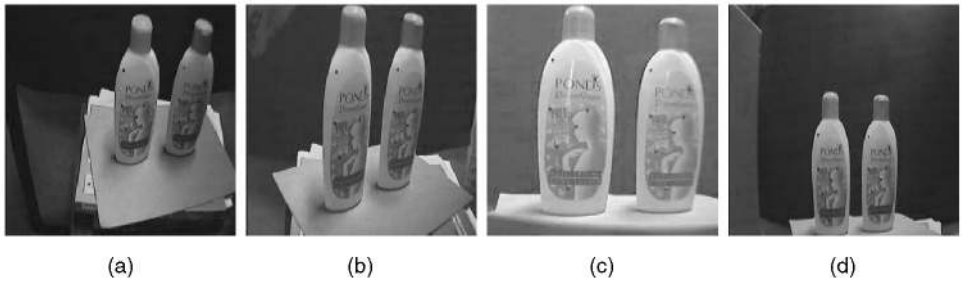

Fig. 12. Views of Scene 2 for stability analysis.

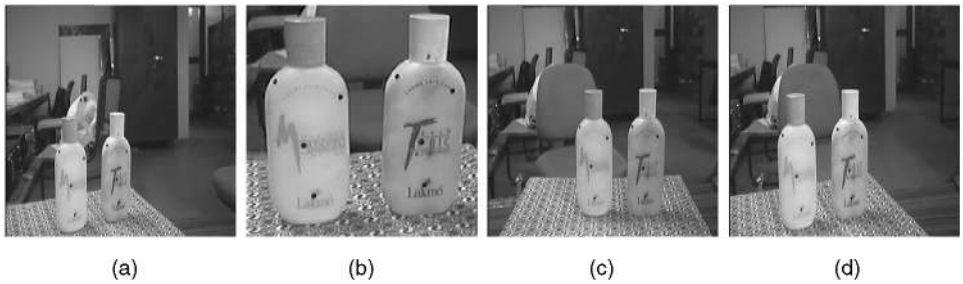

Fig. 13. Views of Scene 3 for stability analysis.

TABLE 6
Distances of Projected Image Vectors from Their Classes

View	Class I	Class II	Class III
11 (a)	2.25	1.5916e6	5.2753e6
11 (b)	2.25	5.7758e6	1.6232e7
11 (c)	2.25	4.9613e6	1.517e7
11 (d)	2.25	5.8980e6	1.6876e7
12 (a)	1.3188e3	2.25	69.2062
12 (b)	1.2623e3	2.25	1.7212e3
12 (c)	1.1992e3	2.25	192.1235
12 (d)	1.1575e3	2.25	266.1613
13 (a)	1.4983e3	15.1453	2.25
13 (b)	1.4213e3	88.2481	2.25
13 (c)	1.4632e3	133.5598	2.25
13 (d)	1.4665e3	78.7997	2.25
14 (a)	1.1823e3	1.1774	221.3684
14 (b)	1.4855e3	14.8133	1.9313
10 (b)	1.3099e3	2.3942	77.9522
	1.1897e3	1.0151	209.7732
	1.1221e3	5.1938	348.7102
	1.2121e3	0.3402	174.3711

particular, have been developed. Joint projective invariants have been proposed for a general pair of proper quadrics. These have been applied for the recognition of quadric configurations from a single image. The reconstruction-based recognition strategy is general and applicable to all repeated objects for which invariants can be computed.

Experiments on real and synthetic images establish the discriminatory power and the stability of these invariants as well as the strategy. We have also considered the application of this technique for recognition of real life objects like historical monuments with multidome architecture. The ability of these invariants in distinguishing images of different historical monuments despite variations in their views, based on their geometric similarity, indicates a possible application of this measure for indexing images in a digital library. For the reconstruction of quadrics, we need the two outline conics and four point correspondences. The strategy would fail in cases when the outline conics are occluded (occlusion to some extent is permissible by Bookstein's algorithm [1]), or if it is not possible to pick image point correspondences, they are not in general position in the image or the points lie on the outline conic. An alternate strategy to handle occlusion has been developed in [4] which takes into account the repetition explicitly.

As an extension of this work, a general reconstruction framework can be developed for affinely repeated objects. The case of translationally repeated objects can then be approached as a special case of that. Proposed approach can also be adapted for analysis of scenes with multiple repeated components.

APPENDIX

We will now establish a relationship between H_Π and H_∞ by the following theorem. This relationship has also been proved by Shashua and Navab [22] and Luong and Vieville [12]. We prove it with respect to our framework.

Theorem 7.1. *Let $\widetilde{P} = K[R_w\ t_w]$ and $\widetilde{P}' = K'[R'_w\ t'_w]$ be the two cameras. Let Π be the reference plane. Then, $H_\Pi = H_\infty + e'_N \nu^t_{\Pi_N}$ where $e'_N = \frac{e'}{\|e'\|}$, the normalized epipole, H_Π is the homography between the two image planes, with respect to the plane Π, and $\nu^t_{\Pi_N}$ is expressed in terms of the coordinates of the plane Π and the internal camera parameters.*

Proof. As we want the expression of k in terms of actual distances, we take the canonical decomposition of the camera matrices in terms of the intrinsic and extrinsic parameters in the form

$$\widetilde{P} = K[R_w\ t_w], \quad \widetilde{P}' = K'[R'_w\ t'_w]. \tag{8}$$

Now,

$$\widetilde{m} = \widetilde{P}M = K[R_w\ t_w] = K(R_w(X\ Y\ Z)^t + t_w).$$

Therefore,

$$K^{-1}\widetilde{m} = R_w(X\ Y\ Z)^t + t_w. \tag{9}$$

Similarly,

$$K'^{-1}\widetilde{m}' = R'_w(X\ Y\ Z)^t + t'_w. \tag{10}$$

Eliminating $(X\ Y\ Z)^t$ between (9) and (10), we get

$$\widetilde{m}' = K'R'_wR_w^{-1}K^{-1}\widetilde{m} + K'(t'_w - R'_wR_w^{-1}t_w).$$

By defining $R'_wR_w^{-1} = R$ and $t'_w - R'_wR_w^{-1}t_w = T$, we get

$$\widetilde{m}' = K'RK^{-1}\widetilde{m} + K'T. \tag{11}$$

By using the form of the camera matrix in (8), we get $H_\infty = P'P^{-1} = (K'R'_w)(KR_w)^{-1} = K'R'_wR_w^{-1}K^{-1} = K'RK^{-1}$. Also, $\widetilde{e}' = -K'R'_wR_w^{-1}t_w + K't'_w = K'(t'_w - Rt_w) = K'T$. Substituting into (11), we get

Fig. 14. Additional views for stability analysis.

$$\widetilde{m}' = H_\infty \widetilde{m} + \widetilde{e}'. \tag{12}$$

Let the normalized coordinates of the plane $\Pi = \begin{pmatrix} l \\ -\delta \end{pmatrix}$, where l is a 3×1 vector.

For a point M lying on the plane Π, $l^t(K^{-1}\widetilde{m}) = \delta$. This gives

$$\frac{l^t(K^{-1}\widetilde{m})}{\delta} = 1. \tag{13}$$

Combining (13) and (12), we get $\widetilde{m} = (H_\infty + \widetilde{e}' \frac{l^t K^{-1}}{\delta})\widetilde{m} = H_\Pi \widetilde{m}$ (since $M \in \Pi$ and $H_\Pi \widetilde{m} = \widetilde{m}'$). This gives

$$\begin{aligned} H_\Pi &= H_\infty + \widetilde{e}' \frac{l^t K^{-1}}{\delta} = H_\infty + \frac{e'}{||e'||} \frac{\lambda_{e'}||e'||l^t K^{-1}}{\delta} \\ &= H_\infty + e'_N \nu^t_{\Pi_N} \qquad (\text{where } \nu^t_{\Pi_N} = \frac{\lambda_{e'}||e'||l^t K^{-1}}{\delta}). \end{aligned} \tag{14}$$

Therefore, we get the desired result $H_\Pi = H_\infty + e'_N \nu^t_{\Pi_N}$.□

Premultiplying by e'^t_N on both sides of (14), we get

$$e'^t_N(H_\Pi - H_\infty) = e'^t_N e'_N \nu^t_{\Pi_N} = ||e'_N||^2 \nu^t_{\Pi_N} = \nu^t_{\Pi_N}.$$

Theorem 7.2. *The following results hold true*

1. $\widetilde{e}' = p' - H_\infty p$.
2. $H_\infty \widetilde{e} = -\widetilde{e}'$.
3. $H_\Pi \widetilde{e} = \gamma \widetilde{e}'$ *for some* $\gamma \in \mathbb{R}$, $\gamma \neq 0$.

Proof.

1. $\widetilde{e}' = [P'\ p'] \begin{pmatrix} -P^{-1}p \\ 1 \end{pmatrix} = -P'P^{-1}p + p' = p' - H_\infty p.$
2. $H_\infty \widetilde{e} = P'P^{-1}[P\ p] \begin{pmatrix} -P'^{-1}p' \\ 1 \end{pmatrix} = P'P^{-1}p - P'P^{-1}PP'^{-1}p' = H_\infty p - p' = -\widetilde{e}'$ (from 1)).
3. From Theorem 7.1, we have $H_\Pi = H_\infty + e'_N \nu^t_{\Pi_N}$. Therefore,

$$\begin{aligned} H_\Pi \widetilde{e} &= H_\infty \widetilde{e} + e'_N \nu^t_{\Pi_N} \widetilde{e} = -\widetilde{e}' + \nu^t_{\Pi_N} \widetilde{e} e'_N \\ &\quad (\text{because } \nu^t_{\Pi_N} \widetilde{e} \text{ is a scalar}) \\ &= -\widetilde{e}' + \nu^t_{\Pi_N} \widetilde{e} \frac{e'}{||e'||} \frac{\lambda_{e'}}{\lambda_{e'}} = \left(-1 + \frac{\nu^t_{\Pi_N} \widetilde{e}}{\lambda_{e'}||e'||} \right) \widetilde{e}' \\ &= \gamma \widetilde{e}' \qquad \left(\text{where } \gamma = \left(-1 + \frac{\nu^t_{\Pi_N} \widetilde{e}}{\lambda_{e'}||e'||} \right) \right). \end{aligned}$$

Now, from (14), $\nu^t_{\Pi_N} = \frac{\lambda_{e'}||e'||l^t K^{-1}}{\delta}$. Using this, $\nu^t_{\Pi_N} \widetilde{e} = \frac{\lambda_{e'}||e'||l^t}{\delta} K^{-1}\widetilde{e} \neq \lambda_{e'}||e'||$ because $\widetilde{e}$ does not lie on the plane Π. This implies that $\gamma \neq 0$. □

ACKNOWLEDGMENTS

The work was done while R. Choudhury was with the Department of Electrical Engineering, IIT Delhi, India.

REFERENCES

[1] F. Bookstein, "Fitting Conic Sections to Scattered Data," *Computer Vision Graphics and Image Processing,* vol. 9, pp. 56–71, 1979.

[2] J.B. Burns, R.S. Weiss, and E.M. Riseman, "The Non-Existance of General-Case View-Invariants," *Geometric Invariance in Computer Vision,* A. Zisserman and J. Mundy, eds., MIT Press, 1992.

[3] R. Choudhury, "Reconstruction Based Recognition of Repeated 3D Objects Using Invariants," PhD thesis, Dept. of Math., Indian Inst. of Technology, Delhi, India, 1999.

[4] R. Choudhury, S. Chaudhury, and J.B. Srivastava, "A Framework for Reconstruction Based Recognition of Partially Occluded Repeated Objects," *J. Math. Imaging and Vision,* vol. 14, pp. 5–20, 2001.

[5] R. Choudhury, J.B. Srivastava, and S. Chaudhury, "A Reconstruction Based Recognition Scheme for Translationally Repeated Quadrics," *Proc. First Indian Conf. Computer Vision, Graphics, and Image Processing,* pp. 101–108, 1998.

[6] G. Cross and A. Zisserman, "Quadric Reconstruction from Dual Space Geometry," *Proc. Sixth Int'l Conf. Computer Vision,* pp. 25–31, 1998.

[7] O. Faugeras, *Three Dimensional Computer Vision—A Geometric Viewpoint.* Cambridge, England: MIT Press, 1993.

[8] D.A. Forsyth, J.L. Mundy, A. Zisserman, A. Heller, and C.A. Rothwell, "Invariant Descriptors of 3D Object Recognition and Pose," *IEEE Trans. Pattern Analysis and Machine Intelligence,* vol. 13, no. 10, pp. 971–991, Oct. 1991.

[9] P. Gros and L. Quan, "Projective Invariants for Computer Vision," Technical Report RT 90 IMAG-15 LIFIA, INRIA, 1992.

[10] D. Heisterkamp and P. Bhattacharya, "Invariants of Families of Coplanar Conics and Their Applications to Object Recognition," *J. Math. Imaging and Vision,* vol. 7, pp. 253–267, 1997.

[11] J. Liu, E. Walker, and J. Mundy, "Characterizing the Stability of 3D Invariants derived from 3D Translational Symmetry," *Proc. Second Asia Conf. Computer Vision (ACCV '95),* 1995.

[12] Q.T. Luong and T. Vieville, "Canonic Representations for the Geometries of Multiple Projective Views," *Computer Vision and Image Understanding,* vol. 64, no. 2, pp. 193–229, 1996.

[13] T. Moons, L. Van Gool, M. Proesmans, and E. Pauwels, "Affine Reconstruction from Perspective Image Pairs with a Relative Object—Camera Translation in Between," *IEEE Trans. Pattern Analysis and Machine Intelligence,* vol. 18, no. 1, pp. 77–83, Jan. 1996.

[14] J.L. Mundy and A. Zisserman, "Repeated Structures: Image Correspondence and 3D Structure Recovery," *Applications of Invariance in Computer Vision,* J.L. Mundy, A. Zisserman, and D. Forsyth, eds., vol. 825, pp. 89–106, 1994.

[15] N. Pillow, S. Utcke, and A. Zisserman, "Viewpoint-Invariant Representation of Generalized Cylinders Using the Symmetry Set," *Image and Vision Computing,* vol. 13, no. 5, pp. 355–365, June 1995.

[16] L. Quan, "Algebraic and Geometric Invariants of a Pair of Non-Coplanar Conics in Space," *J. Math. Imaging and Vision,* vol. 5, pp. 263–267, 1995.

[17] L. Quan, P. Gros, and R. Mohr, "Invariants of a Pair of Conics Revisited," *Image and Vision Computing,* vol. 10, no. 1, pp. 19–23, 1992.

[18] L. Quan and F. Veillon, "Joint Invariants of a Triplet of Coplanar Conics: Stability and Discriminatory Power for Object Recognition," *Computer Vision and Image Understanding,* vol. 70, no. 1, pp. 111–119, 1993.

[19] C. Rothwell, "Recognition Using Projective Invariance," PhD thesis, Univ. of Oxford, 1993.

[20] C. Rothwell, O. Faugeras, and G. Csurka, "A Comparison of Projective Reconstruction Methods for Pairs of Views," *Computer Vision and Image Understanding,* vol. 68, no. 1, pp. 37–58, 1997.

[21] A. Shashua, "Projective Structure from Two Uncalibrated Images :Structure from Motion and Recognition," *IEEE Trans. Pattern Analysis and Machine Intelligence,* vol. 16, no. 8, pp. 778–790, Aug. 1994.

[22] A. Shashua and N. Navab, "Relative Affine Structure: Canonical Model for 3D from 2D Geometry and Applications," *IEEE Trans. Pattern Analysis and Machine Intelligence,* vol. 18, no. 9, pp. 873–883, Sept. 1996.

[23] A. Shashua and S. Toelg, "The Quadric Reference Surface: Theory and Application," *Int'l J. Computer Vision,* vol. 23, no. 2, pp. 185–198, 1996.

[24] A. Zisserman, D.A. Forsyth, J.L. Mundy, C.A. Rothwell, J. Liu, and N. Pillow, "3D Object Recognition Using Invariance," *Artificial Intelligence,* vol. 78, pp. 239–288, 1995.

Ragini Choudhury received the PhD degree from the Indian Institute of Technology, Delhi (India) in the field of computer vision, with the Department of Mathematics in 2000. She received a masters degree in mathematics and a masters of technology in computer applications from the same Institute in 1994 and 1996, respectively. She is currently working as a post doctoral researcher in the field of computer vision with the MOVI team at INRIA, Rhone-Alpes, France. Her research interests include reconstruction and recognition problems in vision, geometry, and tracking.

J.B. Srivastava is a professor in the Department of Mathematics at IIT Delhi. His major area of research is algebra: group rings, group theory, and group theoretical methods. On the applications side, he is currently doing collaborative research work in 3D computer vision and signal processing using group theoretical methods and computational projective geometry.

Santanu Chaudhury received the BTech (Hons.) degree in electronics and electrical communication engineering and the PhD degree in computer science and engineering from the Indian Institute of Technology, Kharagpur in 1984 and 1989, respectively. Currently, he is a professor in the Department of Electrical Engineering at the Indian Institute of Technology, Delhi. He was awarded INSA medal for young scientists by the Indian National Science Academy in 1993. His research interests include Computer Vision, Multimedia Systems, and Artificial Intelligence. He is a member of the IEEE.